Gas Processing Journal

Vol. 10, No. 2, 2022, pp. 25 - 36
http://gpj.ui.ac.ir

Research Paper

Enhancing Gasoline Hydro-Desulfurization in a Fixed Bed Reactor: A Computational Fluid Dynamics (CFD) Study

Abbas Ghareghashi [1*], Abbas Sohrabi [2], Zohreh Rahimi-Ahar [1]

[1] Department of Chemical Engineering, Engineering Faculty, Velayat University, Iranshahr, Iran
[2] Abadan Oil Refinery, Gasoline Post Treatment Unit, Abadan, Iran

Received: 2023-05-09 Revised: 2023-08-01 Accepted: 2023-10-07

Abstract: Gasoline produced from fluid catalytic cracking (FCC) units contains substantial amounts of sulfur, which contributes to pollution. This study focuses on the hydro-desulfurization of gasoline in a fixed-bed reactor using computational fluid dynamics (CFD). The study provides a comprehensive analysis of reactor performance by investigating various parameters such as velocity, pressure, and temperature contours at different sections of the reactor. The visualization of these variations helps understand the hydro-desulfurization process in greater detail and aids in optimizing desulfurization technology. The simulations were conducted and validated results using operational data from the hydrogen refining unit of Abadan Oil Refining Company. The highest temperature was observed along the central line of the reactor, and the maximum pressure drop occurred in the catalytic section. The concentration of hydrogen sulfide (H2S), a product of the hydro-desulfurization reaction, increased by 15-fold and reached 0.008 kmol/m3 as it moves moved from the entrance to the outlet of the reactor. Additionally, the productivity of the reaction, as well as the molar concentration of H2S, increased with an increase in the feed mass flow rate. However, it should be noted that an increase in the feed temperature resulted in higher reaction yields, but it might also lead to the reduced thermal resistance of the catalyst, potentially affecting its effectiveness. Additionally, the concentration of gasoline and hydrogen decreased from the reactor inlet to the outlet, while the concentration of H2S increased.

keywords: hydro-desulfurization, fixed bed reactor, CFD, simulation, gasoline.

1. Introduction

The desulfurization of diesel fuel and gasoline is of great importance due to its significant environmental impact. To comply with world standards and limit pollutant emissions, various measures have been taken to reduce the sulfur content in gasoline. Gasoline is produced through different processes like isomerization, reforming, and fluid catalytic cracking (FCC) units. While gasoline produced in isomerization and reforming units contains little to no sulfur, gasoline from FCC units contains substantial amounts of sulfur [1]. Catalytic hydrotreating, known as hydrodesulfurization (HDS), is a widely used method in refineries to remove sulfur from crude oil products, including gasoline, diesel fuel, kerosene, and fuel oil [2]. Well-calibrated equipment and optimized processes should be applied to produce fewer pollutants and meet standard limits [3]. According to environmental regulations in most countries, the sulfur content in gasoline must be reduced to below 50 parts per million (ppm) [4]. In many countries, ultra-low-sulfur fuels with zero emissions are also mandated, which cannot be achieved through conventional desulfurization processes [5]. Desulfurization is based on two main approaches: hydrodesulfurization (HDS) and non-hydrodesulfurization (non-HDS). Significant advancements have been made in catalysis-based HDS technologies, including improved catalyst synthesis, distillation hybridization, and advanced reactor design [6]. Additionally, non-HDS processes like extraction, precipitation, alkylation, adsorption, and oxidation have also shown considerable progress in sulfur removal from petroleum products. An integrated technology that achieves zero sulfur emissions has been proposed as an effective desulfurization process [7].

However, the conventional catalyst-based HDS process is costly due to its high-temperature and high-pressure reactor and vessel requirements [8]. The desulfurization level depends on various factors, such as the type of catalyst used, its activity and properties,

* Corresponding Author.
Authors' Email Address: [1] A. Ghareghashi (A.ghareghashi@velayat.ac.ir), [2] A. Sohrabi (Sohrabi38abbas@gmail.com), [3] Z. Rahimi-Ahar (z.rahimi@velayat.ac.ir)

http://dx.doi.org/10.22108/GPJ.2023.137639.1129

reaction conditions, sulfur compound concentration in the feed, process design, and reactor configuration. Traditionally, sulfide $NiMo/Al_2O_3$ and $CoMo/Al_2O_3$ catalysts are commonly used in HDS processes, and their selectivity can be improved through specific modifications [9]. It has been observed that the ideal catalysts not only remove sulfur but also improve fuel specifications, such as aromatics content or cetane/octane number, which are crucial for meeting environmental standards and maintaining high fuel quality [6].

Several methods have been explored to decrease or remove sulfur from gasoline, as evidenced by various studies. Tawara et al. [10] used a 12% Ni/ZnO catalyst for HDS of kerosene with a hydrogen and CO_2 stream, achieving a residual sulfur content lower than 0.06 ppm after 800 h of operation. Li et al. [11] utilized β-CD-TiO_2-Ag catalysts in ionic liquids for desulfurization, with the concentration of nanoparticles, process temperature, and time influencing the process efficiency. Fan et al. [12] compared the catalytic performances of composite-based Ni-Mo catalysts with a mechanical mixture for FCC gasoline hydro-upgrading, where the composite catalyst exhibited superior performance. Wu et al. [13] investigated an optimization model that integrated hydrogenation reaction kinetics of the hydrotreating unit and impurity distributions of FCC was built to reduce the utility cost of the process. Furthermore, a modeling approach was applied to enhance the hydrocarbon compositions in gasoline using the structure-oriented lumping method [14].

In the realm of hydro-desulfurization for diesel fuel, various catalysts like $CoMo/CeO_2$, Al_2O_3, and TiO_2 have been studied, with $CoMo/CeO_2$ showing the highest catalytic activity towards hydro-desulfurization [15, 16]. Though the catalyst showed good performance, it is important to note that diesel fuel has different properties than gasoline. The current work focused on gasoline desulfurization, which requires a distinct approach due to its unique composition. CoMo/AMK-850-27 catalysts supported by γ-Al_2O_3 and HZSM-5 have well performed in providing balanced HDS selectivity and activity, excellent octane number, and low cracking performance [17]. Additionally, the modification of ZrO_2-r-Al_2O_3 with indium, nickel, and lanthanum species resulted in a 2-unit increase in the octane number of the product and zero sulfur content [18]. Moreover, the MgO-supported Cu-Ni catalyst showed improved stability to oxidation, while the NaOH-rich catalyst was more resistant to deactivation of the oxidation of thiol [19].

While HDS has been widely used, it comes with the drawbacks of requiring in-situ hydrogen sources, high pressure, and temperature, leading to significant investment costs. As an alternative, oxidative desulfurization (ODS) has been proposed due to its lower hydrogen requirement and mild reaction conditions [20]. Furthermore, the freeze-drying technique has been suggested as a complementary method, capable of providing an adsorbent with a smaller size and enhanced pore structure compared to conventional oven drying [21]. Despite great advancements in gasoline hydro-desulfurization, the underlying mechanisms of this technology have not yet reached satisfying results. Understanding and establishing these mechanisms could play an effective role in enhancing desulfurization technology and optimizing desulfurization sorbents.

This study presents a case study on the hydro-desulfurization of gasoline in a fixed-bed reactor using Computational Fluid Dynamics (CFD). $CoMo/Al_2O_3$ hydro-desulfurization catalysts were employed. The choice of catalysts reflects practical applicability and relevance to large-scale refinery operations. The simulation was validated using operational data from the hydrogen refining unit of Abadan Oil Refining Company. The literature review shows that further investigations are required for industrial-scale gasoline hydro-desulfurization units. The achievement of this work also lies in understanding the behavior of hydro-desulfurization catalysts under realistic conditions for gasoline purification. The study aimed to shed light on key factors influencing the process, such as temperature, pressure, feed flow rate, and catalyst performance, to enhance desulfurization efficiency and gasoline quality. Understanding these aspects could contribute to the development of more cost-effective and environmentally friendly desulfurization technologies for gasoline production.

2. Governing equations

In this study, the velocity and momentum variations were considered using the Brinkman equation. Pressure and fluid velocity are the independent parameters and governing equations in porous media. The continuity and momentum equations are given as follows [22]:

$$\frac{\rho}{\varepsilon_p}\left(\frac{\partial u}{\partial t}+(u.\nabla)\,u\frac{1}{\varepsilon_p}\right)=\nabla.\left[-pI+\mu\frac{1}{\varepsilon_p}(\nabla u+(\nabla u)^T)-\frac{2}{3}\mu\frac{1}{\varepsilon_p}(\nabla.u)I\right]-\left(\frac{\mu}{\kappa}+\beta|u|+\frac{Q_{br}}{\varepsilon_p^2}\right)u+F \quad (1)$$

$$\frac{\partial(\varepsilon_p\rho)}{\partial t}+\nabla.(\rho u)=Q_{br} \quad (2)$$

Where u, ρ, μ, P, ε_p, k, Q_{br}, and F denote fluid velocity, fluid density, the dynamic viscosity of the fluid, pressure, porosity, permeability tensor, source, and body force, respectively.

In this study, the k-ε turbulent model was used using Eqs. (3) and (4) [23,24].

$$\rho\frac{\partial k}{\partial t}+\rho(u.\nabla)\,k=\nabla.\left[\left(\mu+\frac{\mu_T}{\sigma_k}\right)\nabla k\right]+P_k-\rho\varepsilon \quad (3)$$

$$\rho\frac{\partial \varepsilon}{\partial t}+\rho(u.\nabla)\varepsilon=\nabla.\left[\left(\mu+\frac{\mu_T}{\sigma_k}\right)\nabla\varepsilon\right]+C_{\varepsilon1}\frac{\varepsilon}{k}P_k-C_{\varepsilon2}\rho\frac{\varepsilon^2}{k} \quad (4)$$

Where ε and k are the turbulence dissipation rate and turbulence kinetic energy, respectively. Constant coefficients appearing in Eqs. (3) and (4) are tabulated in Table 1.

Table 1. Coefficients of the turbulence model

Item	Value
σ_k	**1**
$C_{\varepsilon2}$	**1.92**
$C_{\varepsilon1}$	**1.44**

Two parameters used in Eqs. (3) and (4) are calculated using the following equations:

$$\mu_T=\rho C_\mu\frac{k^2}{\varepsilon} \quad (5)$$

$$P_k=\mu_T\left[\frac{\nabla u}{\nabla u+(\nabla u)^T}-\frac{2}{3}(\nabla.u)^2\right]-\frac{2}{3}\rho k\nabla.u \quad (6)$$

Diffusion and reaction items are calculated using Eq.

(7) [25].

$$\frac{\partial}{\partial t}(\theta c_i) + u.\nabla c_i = \nabla.\left[D_{e,i}\nabla c_i\right] + R_i \quad (7)$$

Where c_i and R_i are the concentrations of species i and the reaction term.

$D_{e,i}$ is the effective diffusion and is calculated using Eq. (8).

$$D_{e,j} = \frac{\varepsilon_p}{\tau_{F,j}} D_{F,j} \quad (8)$$

$$\tau_{F,j} = \varepsilon_p^{\frac{-1}{3}} \quad (9)$$

The following equations are used for heat transfer studies: The heat transfer balance [25] is written as:

$$(\rho C_p)_{eff}\frac{\partial T}{\partial t} + \rho C_p u.\nabla T = \nabla.(k_{eff}\nabla T) + Q \quad (10)$$

Where ρ, cp, T, t, u, and k are the density of the fluid, heat capacity of the fluid, fluid temperature, time, velocity, and heat transfer coefficient of the fluid. Q denotes a heat source, and k_{eff} and ρ. $C_{p.eff}$ are described as:

$$k_{eff} = \theta_p k_p + \theta_L k \quad (11)$$

$$(\rho C_p)_{eff} = \theta_p \rho_p C_{p,p} + \theta_L \rho C_p \quad (12)$$

Where θ_p and θ_L are the solid and fluid volume fractions, respectively.

$$\theta_p + \theta_L = 1 \quad (13)$$

Boundary conditions in the inlet of the reactor are

$$-\int_{\partial\Omega} \rho(u.n) d_{bc}\, dS = m \quad (14)$$

$$T = T_0 \quad (15)$$

$$c_i = c_{0,i} \quad (16)$$

and at the outlet of the reactor are

$$\left[-pI + \frac{\mu}{\varepsilon_p}(\nabla u + (\nabla u)^T) - \frac{2\mu}{3\varepsilon_p}(\nabla.u)I\right]n = -p_0 n \quad (17)$$

$$-n.(-k\nabla T) = 0 \quad (18)$$

$$-n.D_i\nabla c_i = 0 \quad (19)$$

The reaction rate (Eq. 21) is calculated using Eq. (20. The coefficients (Eqs. 22 and 23) are presented by Gunjal and Ranade [26].

$$RS + H_2 \xrightarrow{Catalytic} RH + H_2S \quad (20)$$

$$r_{HDS} = -\frac{k\, c_{L,H_2}^{0.56} c_{L,S}^{1.6}}{1 + K_{Ad}.c_{L,H_2S}} \quad (21)$$

$$K_{Ad} = 50000\frac{m^3}{kmol} \quad (22)$$

$$k = 2.5\times10^{12}\exp(-19384/T) \quad (23)$$

3. Grid testing and model validation

The 3D geometry of the reactor with meshing is displayed in Fig. 1. The reactor contains two catalytic sections. Table 2 shows the geometry and inlet conditions of the proposed reactor. A grid independence check was applied to evaluate the effects of different grid sizes on the outcomes (outlet fluid velocity from the reactor and reactor temperature). The grid independence was checked through three sets of tetrahedral meshes of 202930, 527583, and 861470 cells, respectively. The last two types of meshes yield similar results concerning outlet fluid velocity from the reactor and reactor temperature. In this study, considering the accuracy of the obtained results and in order to decrease the computational time, a set of 527583 cells was chosen. Mesh density was enhanced near the wall to consider the wall effect on porosity distribution.

The validation was made based on feed and operational conditions presented by data obtained from the hydro-desulfurization process in the fixed-bed reactor of the Abadan refinery, Iran. For validation purposes, all hydrocarbons were considered (RSH) and the average physical properties were used in the simulation. The code was validated by comparing the outlet hydrogen sulfide flow rate from the reactor. The CFD results were compared with the experimental data as tabulated in Table 3. It can be observed that the obtained results show close agreement.

Table 2. Physical characteristics of the reactor

Item	Value	Unit
Height	9100	mm
Diameter	3100	mm
Height of each catalytic section	2625	mm
Catalyst diameter	2-4	mm
Specific surface area of the catalyst	130	m^2/g
Loading density	0.5	Kg/l
Fluid convective heat transfer coefficient	0.1025	$W/m^2.K$
Specific heat capacity	2933	J/kg.K
Heat capacity ratio	1.093	-
Convective heat transfer in porous media	40	$W/m^2.K$
Heat capacity in porous media	880	J/kg.K

Table 3. Data validation

Inlet fluid flow rate (kg/h)	Initial hydrogen sulfide flow rate (kg/h)	Outlet hydrogen sulfide flow rate (kg/h)		Relative error (%)
		Simulation	Experimental	
142333	4.1	303.45	332.5	9.56
118053	1.1	248.21	266.7	7.45
113121	0.7	384.56	423	9.99

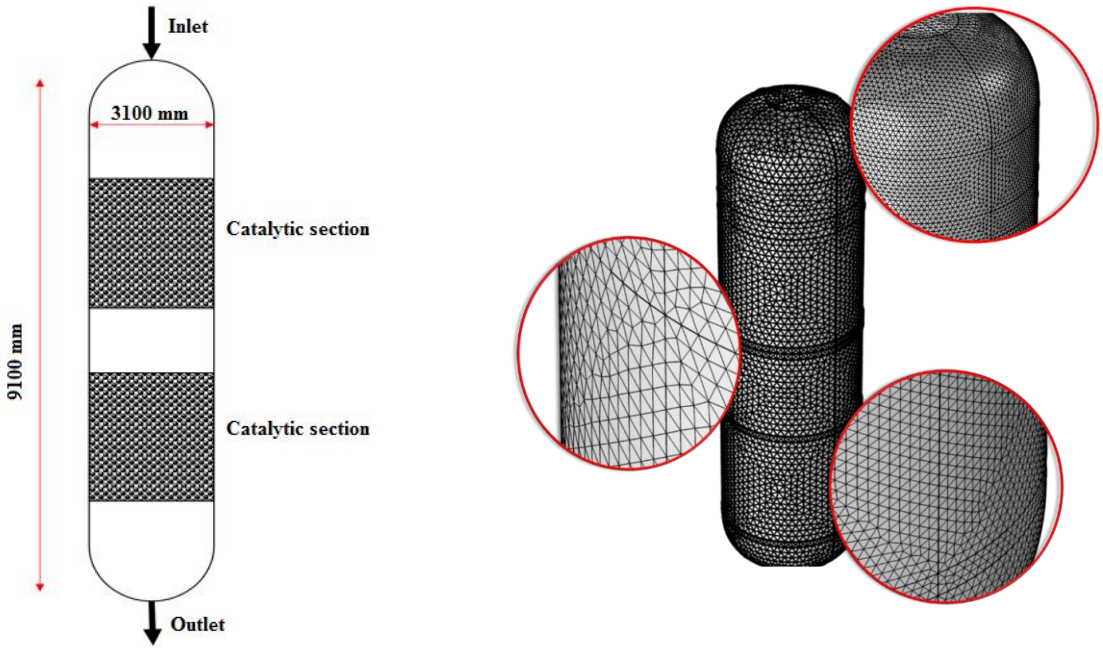

Fig. 1. Dimensions and solution domain of the catalytic fixed bed reactor

The experimental and simulation results were also validated using the feed flow rate and leaving a stream of H_2S in the reactor. Data validation confirmed the simulation procedure as well as gridding the geometry.

4. Gasoline post-treatment unit (GPTU) of Abadan refinery company

GPTU contains three sections, including the selective hydrogenation unit (SHU), splitter (separation of heavy naphtha from the light first unit), and selective desulfurization. The gasoline produced in the FCC unit is the feedstock for the hydro-desulfurization unit. The capacity of this unit is 27000 BPSD. Gasoline stored in a tank in the unit is mixed with hydrogen and enters the SHU. The pressure and temperature in this unit are 24 bar and 160 °C, respectively. After completion of the reaction, it is transferred to the splitter, and the heavy and light naphtha separate. The heavy naphtha has a considerable amount of sulfur that should be desulfurized. It is mixed with a rich hydrogen stream at a temperature range of 260 to 290 °C. This temperature range is produced by the outlet stream from the reactor after the completion of the reaction in a heat exchanger. The HDS reactor is a fixed-bed reactor containing $CoMo/Al_2O_3$ hydrodesulfurization catalysts. The heat produced by the exothermic reaction is carried by the outlet stream from the reactor. This stream is transferred to heat exchangers, which heat the feed stream, and then it is cooled in air coolers. Hydrogen and hydrogen sulfide are separated from gasoline in a separator. This separation process occurs using an amine adsorbent. Hydrogen is returned to the required process cycle, and gasoline flows into the stabilizer tower and its quality is adjusted according to Euro 4 standards. The flow diagram of this unit under Prime G+ technology is presented in Fig. 2.

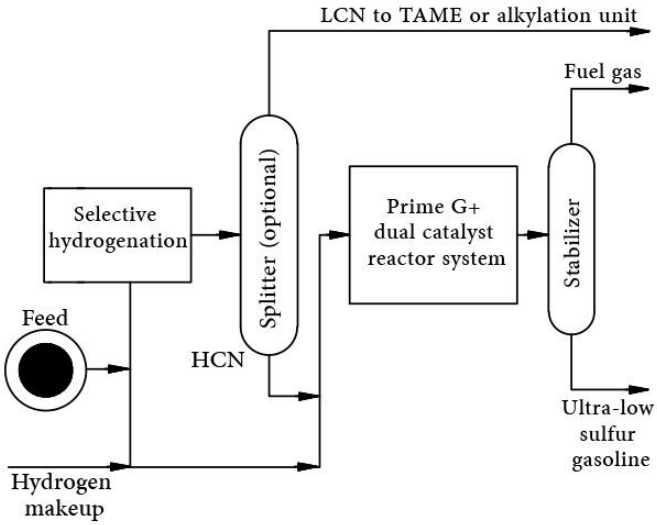

Fig. 2. Flow diagram of the gasoline post-treatment unit (GPTU) of Abadan refinery

5. Results and discussion

The velocity contours at different sections of the reactor are illustrated in Fig. 3. It shows that the feed velocity at the entrance is higher than compared to the other parts of the reactor due to the minimum surface area. As the flowing area increases, the local velocity decreases. At the walls, the velocity follows the no-slip condition and reaches zero. As predicted, the local velocity decreases by moving from the center of the reactor to the wall. In the catalytic section, a uniform velocity distribution is observed which can be due to the Brinkman equations, which show a uniform velocity distribution in porous media.

The pressure contours shown in Fig. 4 confirm that the maximum pressure drop occurs in the catalytic section of the reactor.

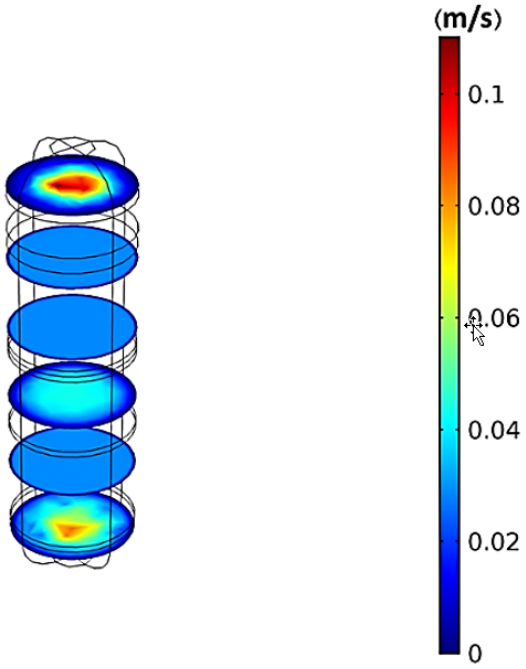

Fig. 3. Velocity variation contours in hydro-desulfurization reactor

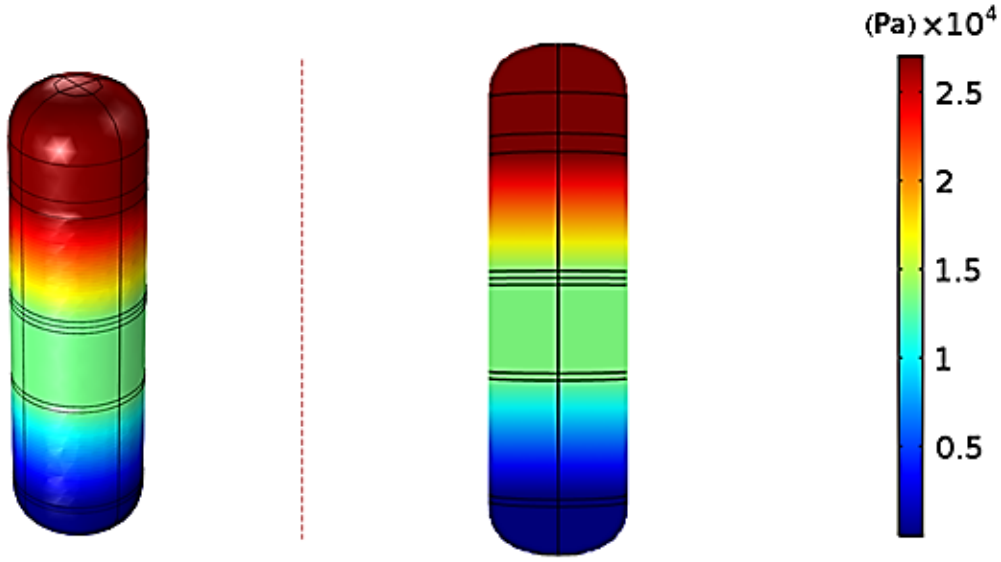

Fig. 4. Pressure variation contours in hydro-desulfurization reactor

A uniform temperature distribution is observed in Fig. 5. Due to the exothermic reaction occurring in the studied hydro-desulfurization reactor, an increase in the temperature is observed along the reactor length. Due to the heat transfer within the inside and outside of the reactor through its wall, a minimum temperature at the walls (200 °C) is obtained. Temperature distribution in different sections of the reactor also confirms a decreased temperature by moving from the center of the reactor to its wall.

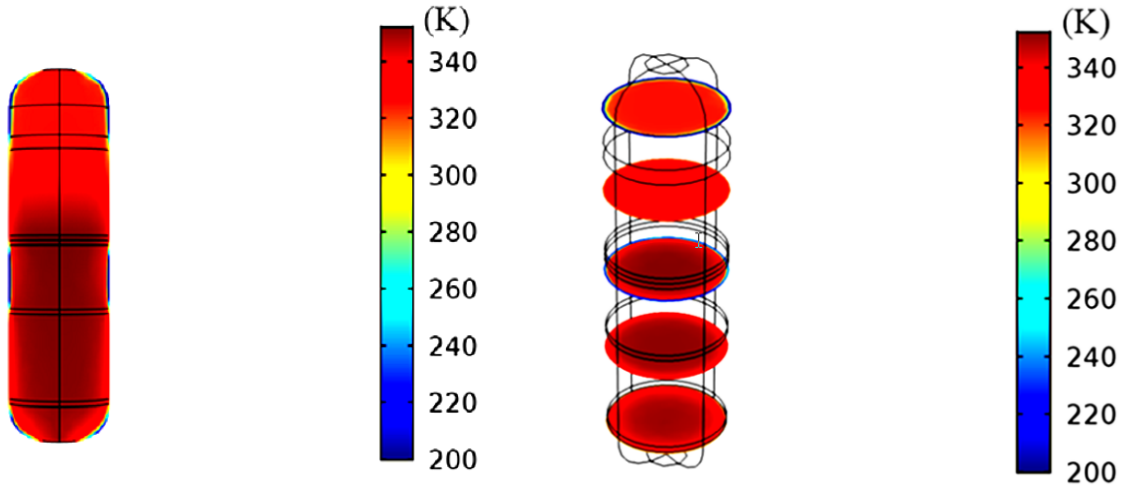

Fig. 5. Temperature variation contours in hydrodesulfurization reactor

Hydrogen concentration variation along with the reactor is shown in Fig. 6A. The hydrogen concentration varies in the porous section of the reactor containing catalysts. In the catalytic section, hydrogen reacts with sulfur, and its concentration decreases. After passing the lower catalytic section of the reactor, the hydrogen concentration becomes constant, and upon entrance into the upper catalytic section, its concentration again decreases. Catalysts ease the desulfurization reaction, and the hydrogen concentration decreases. Hydrogen contours in the wall of the reactor are shown in Fig. 6B. These contours also show the decreasing trend of hydrogen concentration along the reactor. The maximum hydrogen concentration in the center of the reactor leads to an increase in the diffusion coefficient; hence, the maximum mass transfer occurs in the central part of the reaction.

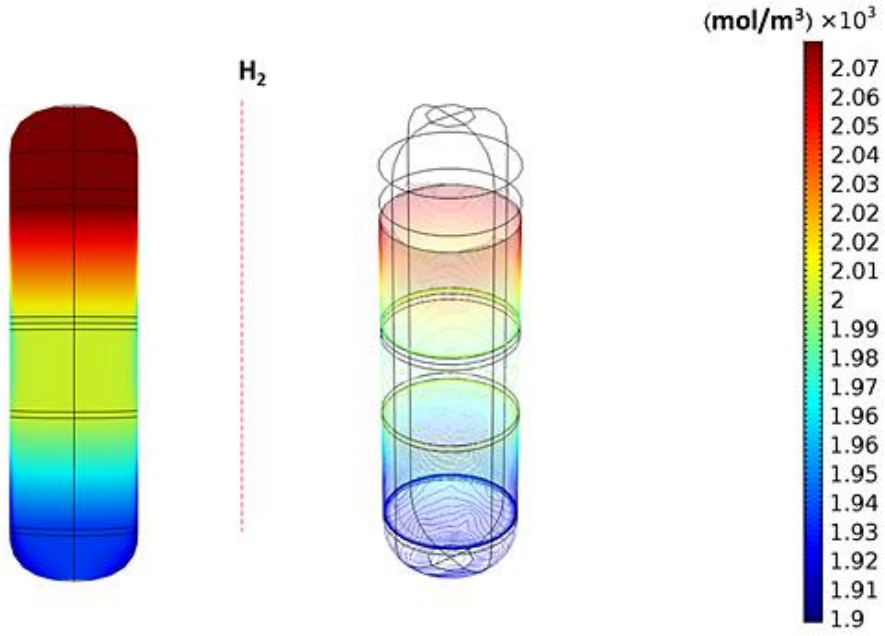

(A) **(B)**

Fig. 6. Hydrogen concentration variation contours in (A) hydro-desulfurization reactor and (B) wall of the reactor

Fig. 7 shows the variation in the gasoline concentration in the reactor. As the hydrogen concentration decreases, the gasoline concentration also decreases. This reduction is not significant; hence, it can be claimed that the gasoline concentration is fixed as the process progresses. This can lead to the desulfurization of gasoline.

The variation in the concentration of H_2S in the hydro-desulfurization reactor is shown in Fig. 8. As predicted, its concentration increases from the entrance to the exit of the reactor, while it is unchanged in non-catalytic sections.

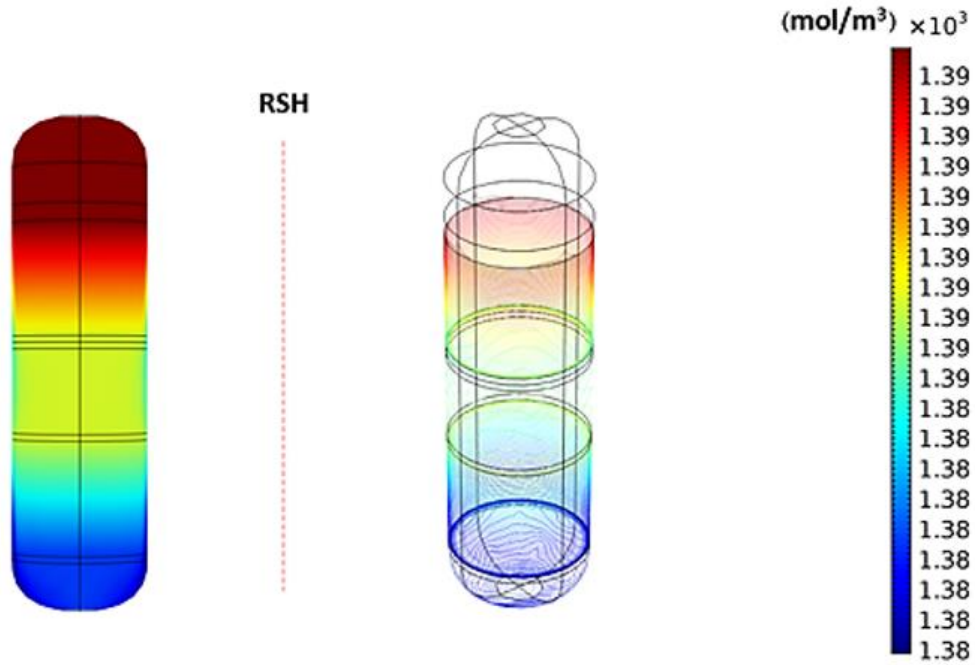

Fig. 7. Gasoline concentration variation contours in hydrodesulfurization reactor

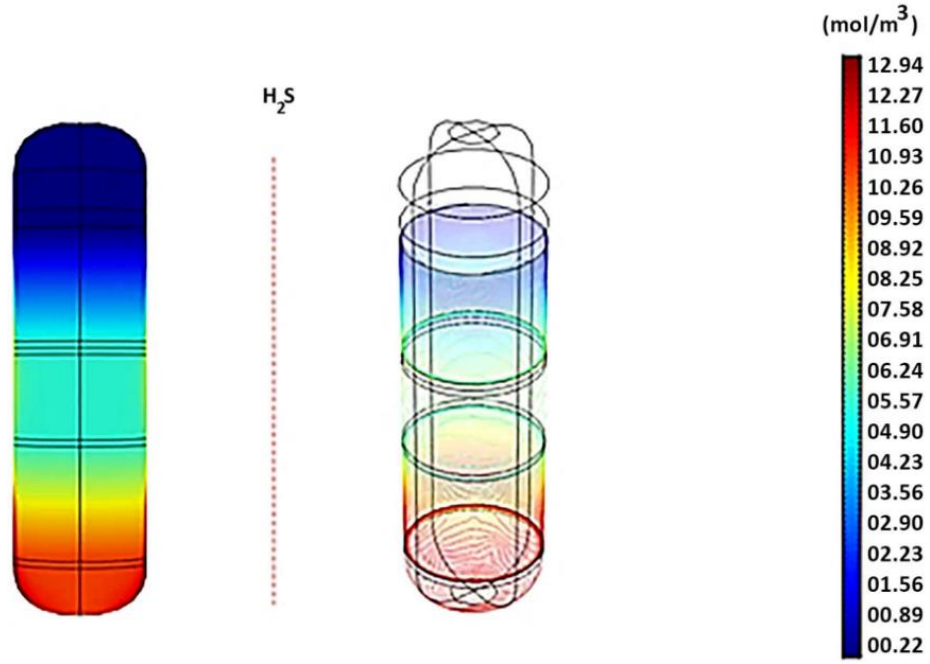

Fig. 8. Hydrogen sulfide concentration variation contours in hydrodesulfurization reactor

The variation in the hydrogen concentration along the central line of the reactor is shown in Fig. 9. It decreases by about 5% in two catalytic sections, while it does not change in non-catalytic sections due to non-reactant existence. A similar trend in variation in gasoline concentration is also observed (Fig. 10). A 0.3% reduction in its concentration is concluded after the completion of the reaction.

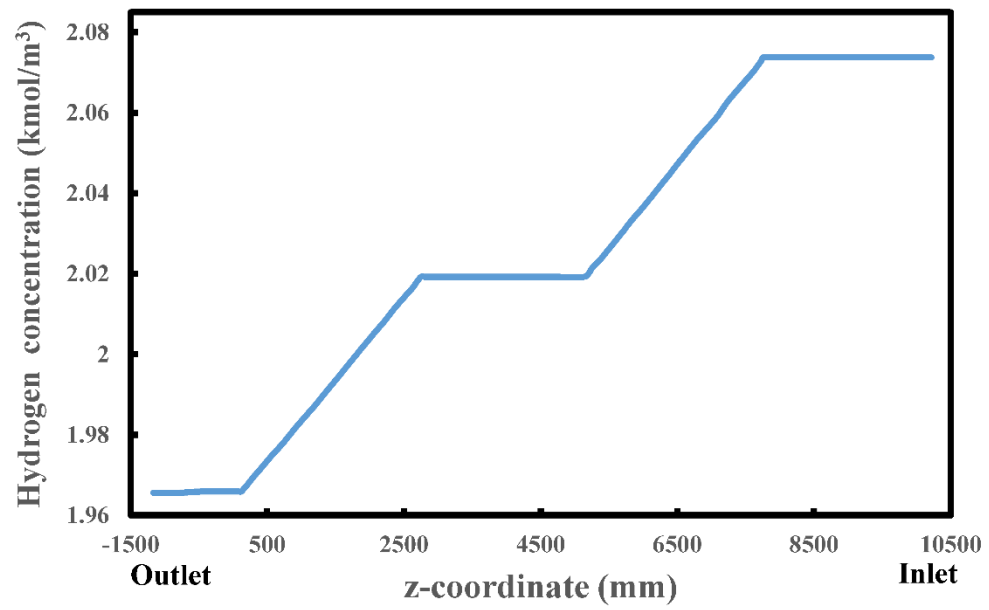

Fig. 9. Hydrogen concentration change in the central line of the hydro-desulfurization reactor

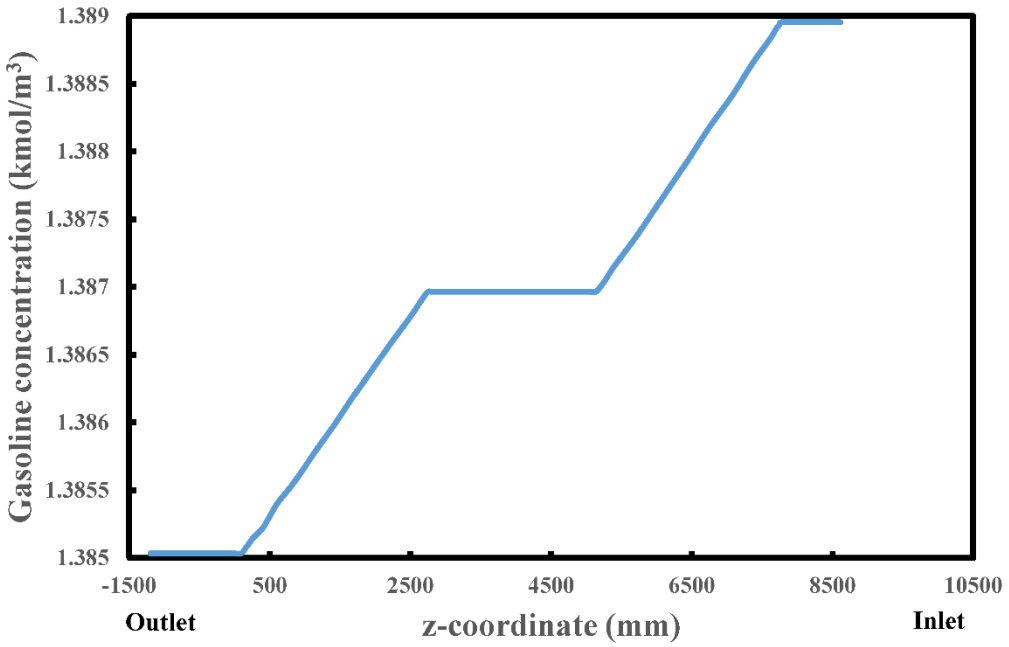

Fig. 10. Gasoline concentration change in the central line of the hydro-desulfurization reactor

Fig. 11 presents the variation in the concentration of H_2S (as a product of hydro-desulfurization reactions) in the central line of the reactor. It has its minimum amount at the entrance of the reactor while increasing by moving to the outlet of the reactor. It increases by 15-fold and reaches 0.008 kmol/m^3. After passing the catalytic section of the bed, it has a constant value.

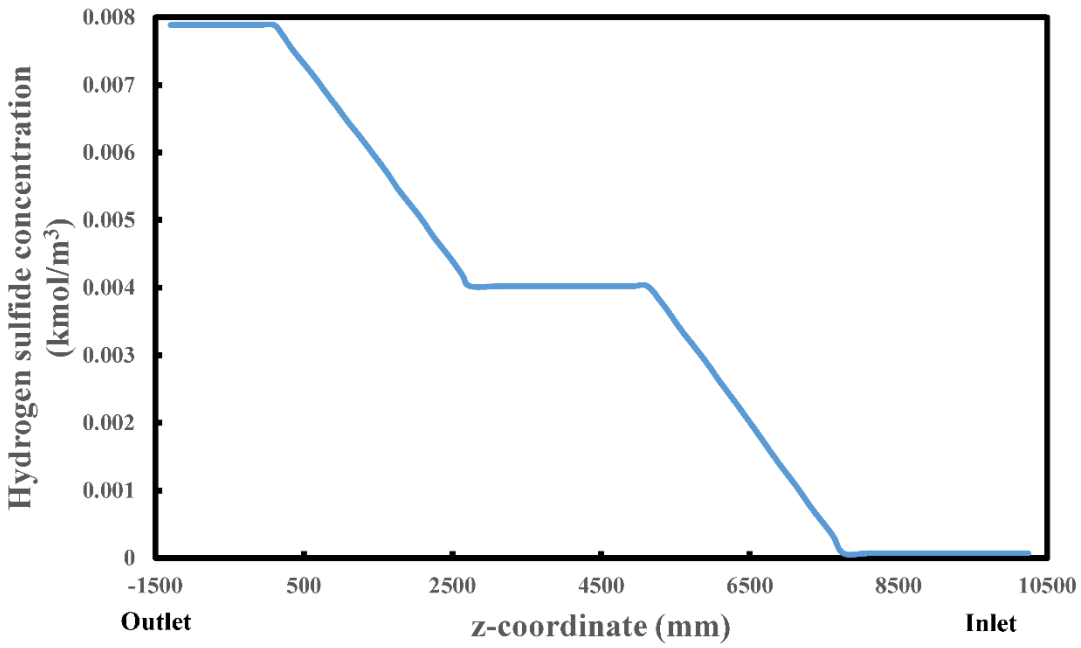

Fig. 11. Hydrogen sulfide concentration variation in the central line of the hydro-desulfurization reactor

The feed mass flow rate affects the velocity of the product of the reactor and the molar concentration of H_2S. By increasing the feed mass flow rate, productivity also increases. In the studied range of the feed mass flow rate, the concentration of H_2S decreases. It means a lower amount of the gasoline containing sulfur reacts in the reactor due to the lower residence time of the hydrogen and gasoline for an effective reaction. It can be concluded that a lower amount of sulfur is separated from gasoline by an increase in the feed flow rate entering the reactor (Fig. 12).

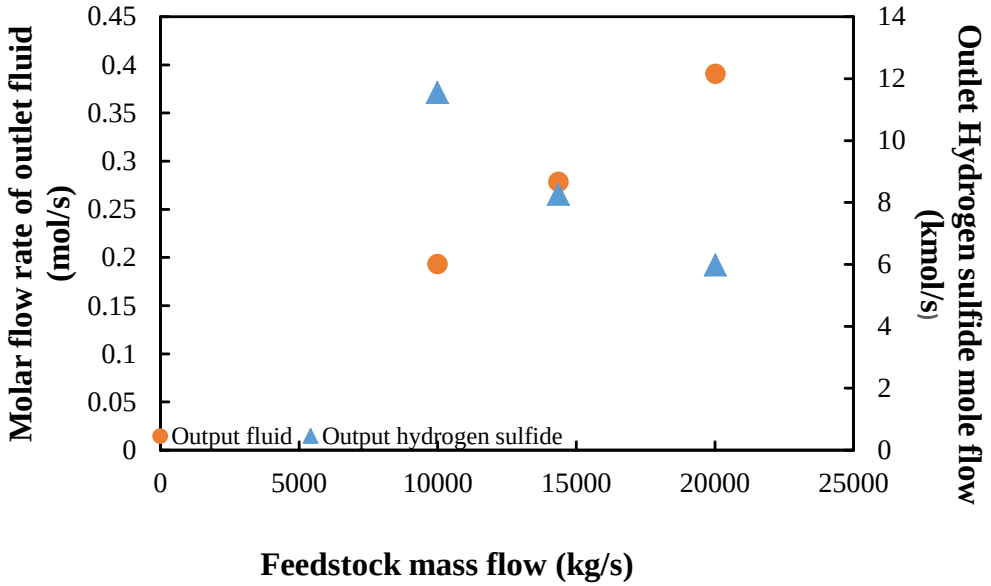

Fig. 12. Variation in the products of the gasoline desulfurization process by the mass flow rate of the feed

The effect of the feed temperature on the product of the gasoline desulfurization process is shown in Fig. 13. By increasing the feed temperature, the fluid temperature in the reactor increases, increasing the reaction yield. It is true that according to the modeling, the progress of the reaction increases with increasing temperature, but it should be noted that at this temperature the catalyst may lose its thermal resistance, and it can be claimed that it will no longer be effective.

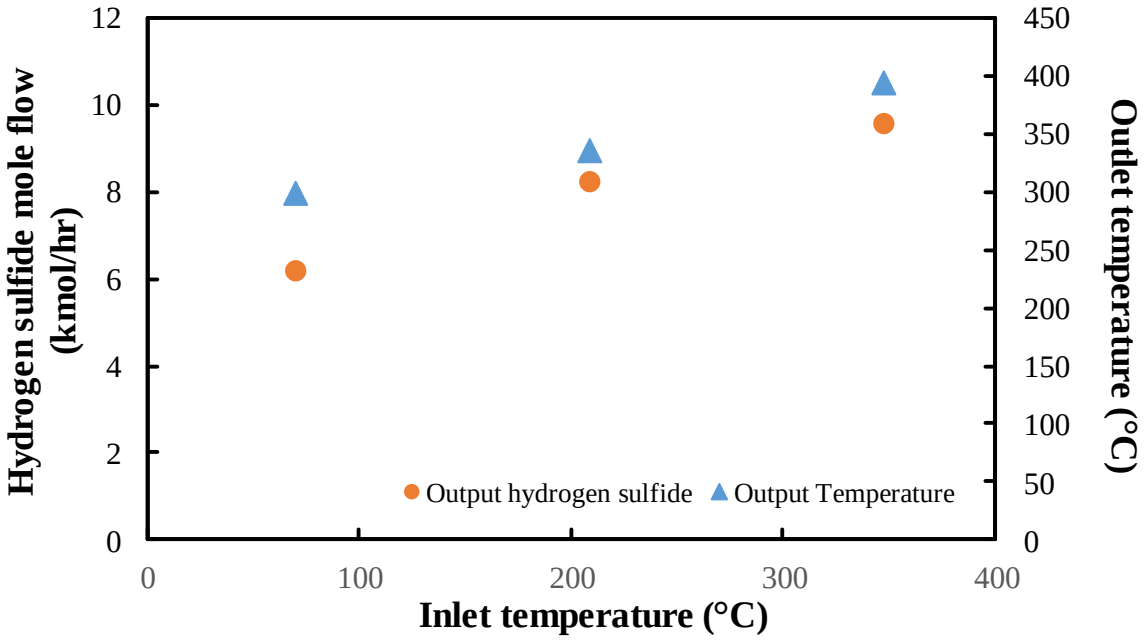

Fig. 13. Variation in the temperature of the products of the gasoline desulfurization process and hydrogen sulfide productivity by feed temperature

Much research has been done on CFD modeling of process reactors. including these works: Harter et al. [27] qualitatively analyzed two-phase flow distribution in trickle-flow catalytic reactors. Three methods were developed to optimize two-phase flow through the catalyst bed. A CFD tool was used to design the inlet gas-liquid distributor, and a collecting device and gamma-ray tomography system were used to measure the liquid flow rate and retention inside the catalyst bed. These methods help design and test reactor inlet distributors. Gunjal and Ranade [26] suggested modeling chemical industry trickle bed reactors (TBRs) with CFD. Flow mal-distribution, catalyst wetting, and design complexity make TBR scale-up difficult. Hydro-processing reactions are simulated using a CFD model in laboratory- and commercial-scale reactors. Experimental data validates the model's performance, which reveals how porosity distribution, particle characteristics, and reactor scale affect TBR performance. CFD modeling can address scaling issues and improve understanding of TBR hydrodynamics and chemical reactions. Wei et al. [28] examined industrial gas-liquid-solid packed-bed reactors' complexity. The study investigated liquid mal-distribution at the micro-level in the packed bed reactor using CFD simulations with a volume of fluid (VOF) model. The research showed how local liquid coverage and liquid holdup on individual particles affect reactor performance, flow hysteresis, and the potential to improve reactor efficiency. Luhaibo et al. [29] presented a Fischer-Tropsch to olefin (FTO) pilot bubbling process model. The model enhanced the gas-liquid-solid FTO reaction by combining single-size microbubbles with millimeter-scale large bubbles. Simulations showed that 50% microbubble intake optimizes catalyst mixing, mass transfer rate, and FTO reaction, resulting in a 40% CO conversion rate 10% higher than without microbubbles. The model's results suggested FTO reaction intensification and improvement.

All these researches are very valuable, while the current study directly addresses the important issue of hydro-desulfurization in gasoline, which is highly relevant for environmental and fuel quality concerns. The use of CFD to study the hydro-desulfurization process in a fixed-bed reactor is a robust approach to understand the reactor's behavior and optimizing desulfurization technology. The research provided a comprehensive analysis of various parameters such as velocity, pressure, temperature, and concentration of H_2S along the reactor, leading to a detailed understanding of the process. The validation of the simulation results using operational data from a real hydrogen refining unit enhances the credibility and applicability of your study.

6. Conclusion

Gasoline is one of the most widely used products in the world, but it also causes a lot of pollution. In this study, hydro-desulfurization of the gasoline process in a fixed-bed reactor was simulated using CFD. The simulation was performed using the operational data of the hydrogen refining unit of Abadan Oil Refining Company. The following conclusions can be expressed according to the obtained results:

- The maximum temperature and pressure drop were at the central line of the reactor and the catalytic section, respectively.
- Velocity at the entrance of the reactor had its maximum value due to the lowest entrance area compared to the body of the reactor.
- From the inlet to the outlet of the reactor, the concentrations of gasoline and hydrogen decreased while the concentration of H_2S increased.
- An increase in the feed temperature led to an increase in the yield, while augmentation of the feed mass flow rate had the opposite result.

The results of each investigation must be analyzed considering the physics of the problem, and without paying attention to the physics of the problem, a wrong

interpretation will reveal itself. Moreover, it is recommended to pay attention to the side reactions of hydro-denitrogenation, isomerization, and hydrogenation.

Conflict of Interest. The authors declare that they have no conflicts of interest.

Reference

Zhao, L., Chen, Y., Gao, J., Chen, Y. (2010). Desulfurization mechanism of FCC gasoline: A review. Frontiers of Chemical Engineering in China, 4, 314-321. https://doi.org/10.1007/s11705-009-0271-9.

Speight, J.G. (2020). Desulfurization, denitrogenation, and demetalization. The Refinery of the Future (Second Edition). 257-301. https://doi.org/10.1016/B978-0-12-816994-0.00008-7.

Zadghaffari, R., Moghaddas, J. S., Rahimiahar, Z. (2012). Numerical investigation of a burner configuration to minimize pollutant emissions. APCBEE Procedia, 3, 177-181. https://doi.org/10.1016/j.apcbee.2012.06.066.

Gasoline Sulfur Octane Fuel Efficiency - Stratas Advisors, 2022.

Kou, J., Lu, C., Sun, W., Zhang, L., Xu, Z. (2015). Facile fabrication of cuprous oxide-based adsorbents for deep desulfurization. ACS Sustainable Chemistry and Engineering, 3 (12), 3053-3061. https://doi.org/10.1021/acssuschemeng.5b01051..

Babich, I. V., Moulijn, J. A. (2003). Science and technology of novel processes for deep desulfurization of oil refinery streams: a review. Fuel, 82 (6), 607-631. https://doi.org/10.1016/S0016-2361(02)00324-1. https://doi.org/10.1016/S0016-2361(02)00324-1.

Gates, B. C., Katzer, J. R., Schutt, O. C. A., Chemistry of. Catalytic Processes, McGraw Hill, New York, 1979.

Lü, H., Zhang, Y., Jiang, Z., Li, C. (2010). Aerobic oxidative desulfurization of benzothiophene, dibenzothiophene and 4, 6-dimethyldibenzothiophene using an Anderson-type catalyst [(C 18 H 37) 2 N (CH 3) 2] 5 [IMo 6 O 24]. Green Chemistry, 12 (11), 1954-1.

Zhang, C., Liu, X., Liu, T., Jiang, Z., Li, C. (2019). Optimizing both the CoMo/Al2O3 catalyst and the technology for selectivity enhancement in the hydrodesulfurization of FCC gasoline. Applied Catalysis A: General, 575, 187-197. https://doi.org/10.1016/j.apcata.2019.02.025.

Tawara, K., Nishimura, T., Iwanami, H. (2000). Ultra-deep hydrodesulfurization of kerosene for fuel cell system (part 2) regeneration of sulfur-poisoned nickel catalyst in hydrogen and finding of auto-regenerative nickel catalyst. Journal of the Japan Petroleum Institute, 43 (2), 114-120.

Li, W., Zou, C. (2018). Deep desulfurization of gasoline by synergistic effect of functionalized β-CD-TiO2-Ag nanoparticles with ionic liquid. Fuel, 227, 141-149. https://doi.org/10.1016/j.fuel.2018.04.083.

Fan, Y., Lei, D., Shi, G., Bao, X. (2006). Synthesis of ZSM-5/SAPO-11 composite and its application in FCC gasoline hydro-upgrading catalyst. Catalysis Today, 114 (4), 388-396. https://doi.org/10.1016/j.cattod.2006.02.050.

Wu, L., Yan, T., Lei, Q., Zhang, S., Wang, Y., Zheng, L. (2022). Operational optimization of co-processing of heavy oil and bio-oil based on the coordination of desulfurization and deoxygenation. Energy, 239, 122558. https://doi.org/10.1016/j.energy.2021.122558.

Qin, X., Ye, L., Liu, J., Xu, Y., Murad, A., Ying, Q., Shen, H., Wang, X., Hou, L., Pu, X., Han, X., Li, J., Wang, R., Liu, N. (2023). A molecular-level coupling model of fluid catalytic cracking and hydrotreating processes to improve gasoline quality. Chemical Engineering Journal, 451, 138778. https://doi.org/10.1016/j.cej.2022.138778.

Ishutenko, D., Anashkin, Y., Nikulshin, P. (2019). The effect of carrier in KCoMoS-supported catalysts for hydro-upgrading of model FCC gasoline. Applied Catalysis B: Environmental, 259, 118041. https://doi.org/10.1016/j.apcatb.2019.118041.

Kim, H. K., Lee, C. W., Kim, M., Oh, J. H., Song, S. A., Jang, S. C., Yoon, C. W., Han, J., Yoon, S. P., Nam, S. W., Choi, D. K., Shul, Y., Ham, H. C. (2016). Preparation of CoMo/Al2O3, CoMo/CeO2, CoMo/TiO2 catalysts using ultrasonic spray pyrolysis for the hydro-desulfurization of 4, 6-dimethyldibenzothiophene for fuel applications. International Journal of Hydrogen Energy, 41 (41), 18846-18857 https://doi.org/10.1016/j.ijhydene.2016.06.040.

Zhang, H., Yang, L., Yang, P., Wang, P., Yue, Y., Wang, T., Bao, X. (2022). CoMoS/modified-kaolin bi-functional hydrodesulfurization-olefin skeletal isomerization catalyst for FCC naphtha hydro-upgrading. Fuel, 324, 124705. https://doi.org/10.1016/j.fuel.2022.124705.

Wang, L., Liu, Q., Jing, C., Yin, J., Mominou, N., Li, S. (2018). Simultaneous removal of sulfides and benzene in FCC gasoline by in situ hydrogenation over NiLaIn/ZrO2-r-Al2O3. Journal of Hazardous Materials, 342, 758-769. https://doi.org/10.1016/j.jhazmat.2017.09.003, https://doi.org/10.1016/j.jhazmat.2017.09.003.

Zhang, Y., Liu, Z., Wang, W., Cheng, Z., Shen, B. (2013). Research on the MgO-supported solid-base catalysts aimed at the sweetening of hydrogenated gasoline. Fuel Processing Technology, 115, 63-70. https://doi.org/10.1016/j.fuproc.2013.03.046.

Mirshafiee, F., Movahedirad, S., Sobati, M. A., Alaee, R., Zarei, S., Sargazi, H. (2023). Current status and future prospects of oxidative desulfurization of naphtha: a review. Process Safety and Environmental Protection, 170, 54-75. https://doi.org/10.1016/j.psep.2022.11.080.

Ullah, R., Bai, P., Wu, P., Etim, U. J., Zhang, Z., Han, D.,Subhan, F., Ullah, S., Roof, M., Yan, Z. (2017). Superior performance of freeze-dried Ni/ZnO-Al2O3 adsorbent in the ultra-deep desulfurization of high sulfur model gasoline. Fuel Processing Technology, 156, 505-514. https://doi.org/10.1016/j.fuproc.2016.10.022.

White, F. M. (2003). Fluid Mechanics 5th edition McGraw Hill Book Company. New York, USA, 52-78.

Bates, P. D., Lane, S. N., Ferguson, R. I. (2005). Computational fluid dynamics: applications in environmental hydraulics. John Wiley & Sons.

Wilcox, D. C. (1998). Turbulence modeling for CFD. La Canada, CA: DCW industries, 2, 103-217.

Sheikholeslami, M. (2018). CuO-water nanofluid flow

due to magnetic field inside a porous media considering Brownian motion. Journal of Molecular Liquids, 249, 921-929. https://doi.org/10.1016/j.molliq.2017.11.118.

Gunjal, P. R., Ranade, V. V. (2007). Modeling of laboratory and commercial scale hydro-processing reactors using CFD. Chemical Engineering Science, 62 (18-20), 5512-5526. https://doi.org/10.1016/j.ces.2007.01.078.

Harter, I., Boyer, C., Raynal, L., Ferschneider, G., & Gauthier, T. (2001). Flow distribution studies applied to deep hydro-desulfurization. Industrial & engineering chemistry research, 40(23), 5262-5267. https://doi.org/10.1021/ie001143x

Du, W., Zhang, J., Lu, P., Xu, J., Wei, W., He, G., & Zhang, L. (2017). Advanced understanding of local wetting behaviour in gas-liquid-solid packed beds using CFD with a volume of fluid (VOF) method. Chemical Engineering Science, 170, 378-392. https://doi.org/10.1016/j.ces.2017.02.033

Zhao, L., Wang, T., Zhang, Y., & Tang, Z. (2022). Modeling Fischer–Tropsch to Olefins in Pilot Slurry Process with a Method of Multiscale Bubbles Hybrid Injection. Industrial & Engineering Chemistry Research, 61(48), 17674-17685. https://doi.org/10.1021/acs.iecr.2c02995